LIÈGE université
SPHERES

GIRPAS
InfraRed Group of
Atmospheric & Solar Physics

BIRA·IASB
aeronomie·be

Observed and simulated atmospheric inorganic fluorine: short-term and long-term trends related to circulation changes

Prignon, M., Bernath, P. F., Chabrillat, S., Chipperfield, M. P., Dhomse, S., Feng, W., Servais, C., Smale, D. and Mahieu E.
PhD student (sup. Emmanuel Mahieu), GIRPAS, ULiège, Belgium
42nd Atmospheric Chemistry Experiment Science Meeting, 15th October 2020

Outline

- Short review of the **Brewer-Dobson circulation**
- **DATA**
  - Ground-based FTIR (Jungfraujoch and Lauder, NDACC)
  - ACE-FTS
  - Chemistry-transport models
    - TOMCAT
    - BASCOE-CTM driven by modern reanalyses
- **F_y** above Jungfraujoch and Lauder
- **Trends**
  - **2D** time-series
  - **Zonal** mean
- **Discussion and conclusion**

Brewer-Dobson Circulation

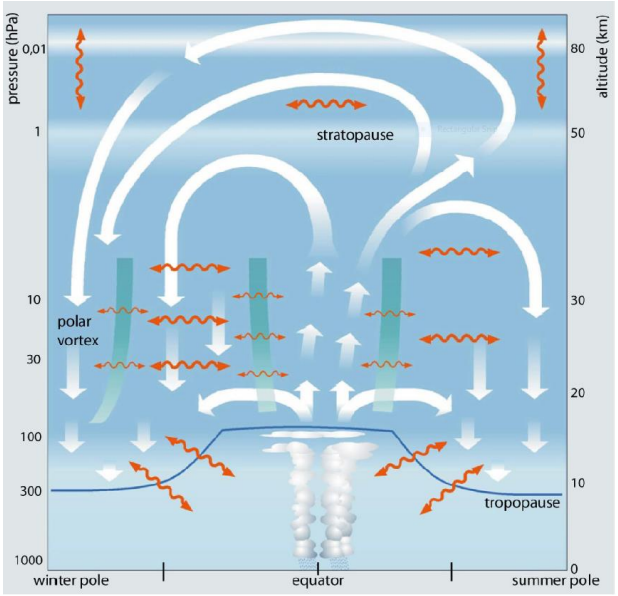

Bönisch et al., 2011, ACP

- Overturning residual circulation (white arrows)
  - Deep branch from tropical tropopause to winter pole by higher parts of the stratosphere
  - Shallow branch in the lower stratosphere from tropical tropopause to higher latitudes (both winter and summer hemispheres)
- Quasi-horizontal two-way mixing (wavy orange arrows)
  - Inhibited at the polar vortex and tropic edges of the winter hemispheres by "transport barriers" (green wide lines) → delimiting the "surf zone"

- Projected to **speed-up** by CCMs in response to increasing GHGs
- Also expected to **slow-down** with most of the changes in the **SH** in response to ozone recovery (2000 →) (e.g., Abalos et al., JGR, 2019; Polvani et al., JGR, 2019)
- In addition to these long-term changes is also observed a **short-term interannual variability** (~5- to 7-year period; e.g., Strahan et al, GRL, 2020)

DATA: Ground-based FTIR

- Jungfraujoch (Switzerland, 46.55° N)
  - From 1989
  - HF (Duchatelet et al., JGR, 2010)
    - 4038.81-4039.07 cm^{-1}
  - COF_2 (Duchatelet et al., ACP, 2009)
    - 1936.15–1936.34 cm^{-1}
      1951.89–1952.05 cm^{-1}
      1952.62–1952.78 cm^{-1} } InSb detector
    - 1230.75–1231.20 cm^{-1}
      1233.90–1234.20 cm^{-1}
      1234.35–1234.63 cm^{-1} } MCT detector
    - Following the multi-spectrum fitting approach
- Lauder (New-Zealand, 45.04° S)
  - From 1999
  - HF
    - 4038.81-4039.07 cm^{-1}
      4109.77-4110.07 cm^{-1}
  - COF_2
    - MCT windows only
    - Monthly coadded spectra → limited to monthly sampling

COClF is currently not retrieved in any FTIR NDACC site

→$*F_y = [HF] + 2x[COF_2]$

DATA: ACE-FTS

- Version 4.0 of level 2 data
  - HF, COF_2 and COClF
- Outliers filtered following Sheese et al. (AMT, 2015)

  Expectation Density Function + 15-day running median and MeAd

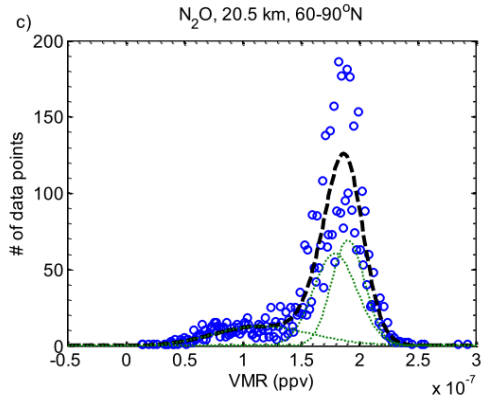

Figure 4. Sunrise ACE-FTS VMR distribution (blue circles) and fitted EDF (black dashed lines) for: **(a)** NO_2 at 30.5 km in the latitude region 60–90° S; **(b)** CH_4 at 20.5 km, 0-60° N; and **(c)** N_2O at 20.5 km, 60–90° N. The dotted green lines are the fitted Gaussian distributions in calculating each of the EDFs, and the fitted distributions have been normalized to the measured VMR distributions.

Sheese et al. (AMT, 2015)

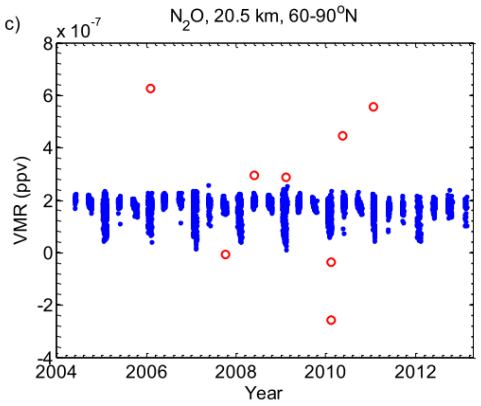

Figure 5. Sunrise ACE-FTS data for the same data subsets as Fig. 4. The red circles are data that have been determined to be unnatural outliers as per the EDFs, and the blue dots are the inlying data.

DATA: Chemistry-transport models

- TOMCAT (University of Leeds, UK)
  - Used to support evaluation of F_y reservoir time-series
- BASCOE-CTM (BIRA-IASB, Belgium)
  - Driven by main modern meteorological reanalyses:
    - ERA-Interim, JRA-55, MERRA, MERRA-2 and ERA5(.1)
  - Lower boundary conditions from Meinshausen et al. (GMD, 2017, 2020)
  - Limited fluorine chemistry where F_y sources are directly decomposed into a F_y tracer

F_y reservoirs

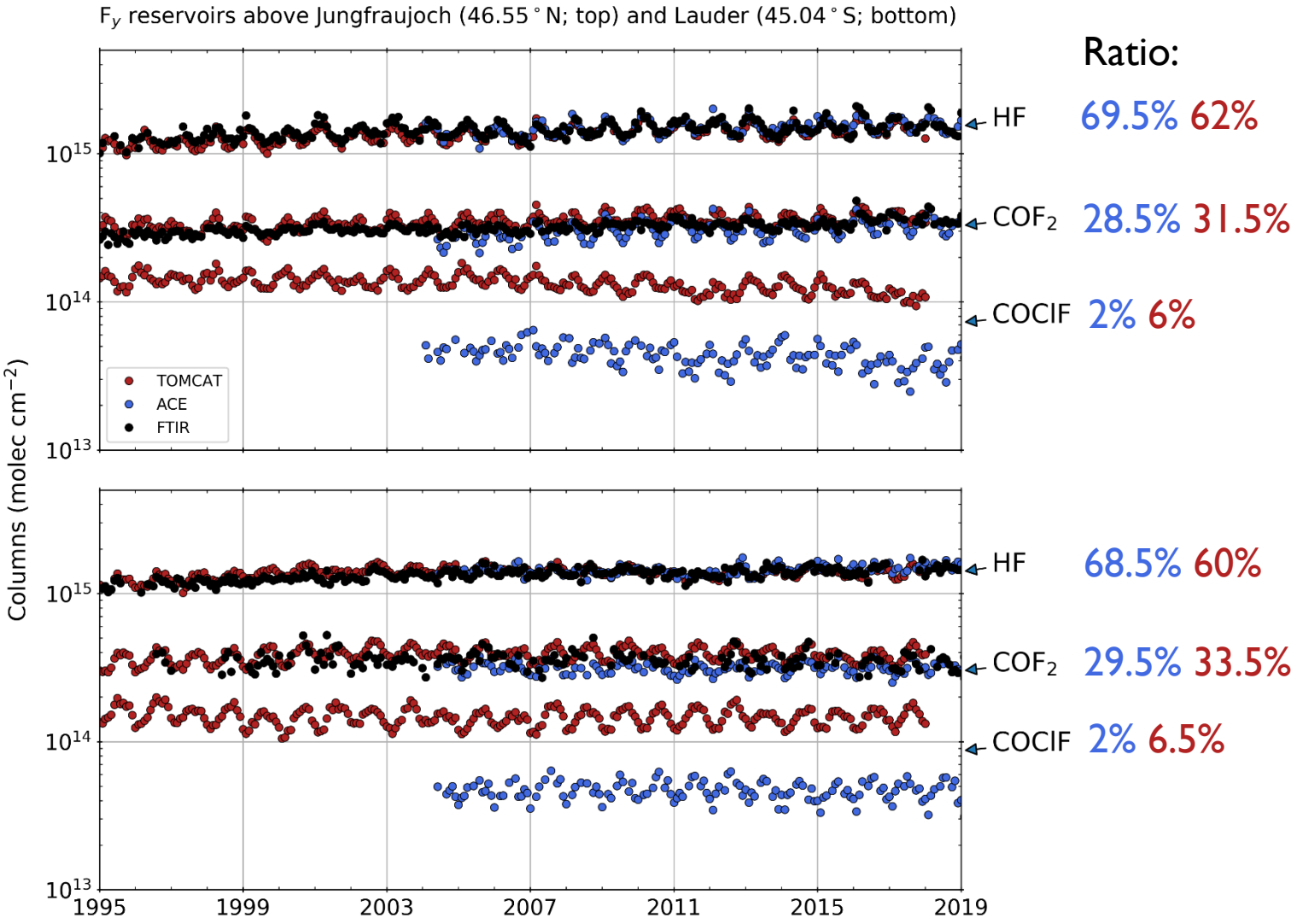

Ratio:

HF 69.5% 62%

COF_2 28.5% 31.5%

COCIF 2% 6%

HF 68.5% 60%

COF_2 29.5% 33.5%

COCIF 2% 6.5%

*F_y above Jungfraujoch and Lauder

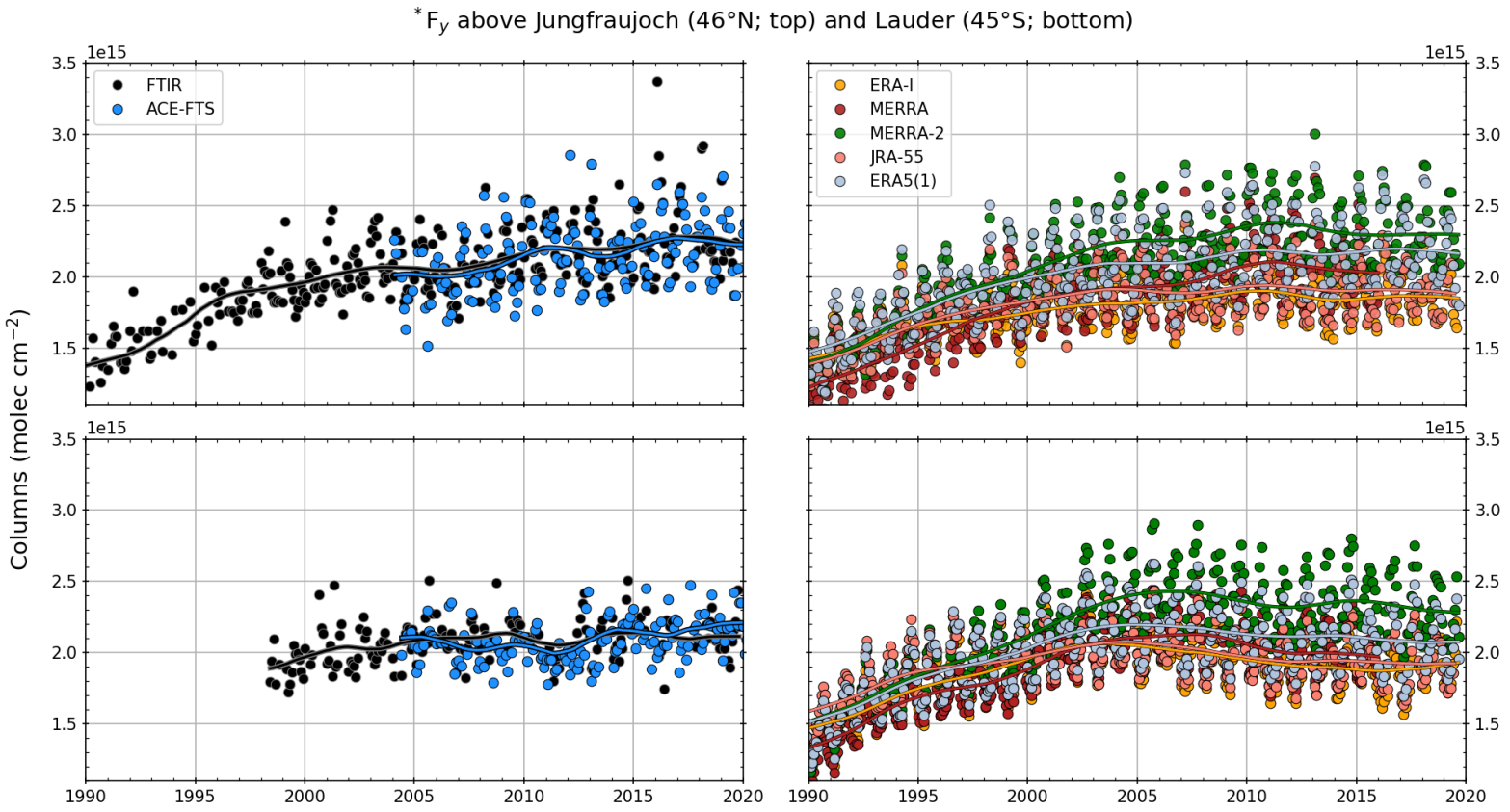

Long-term trends

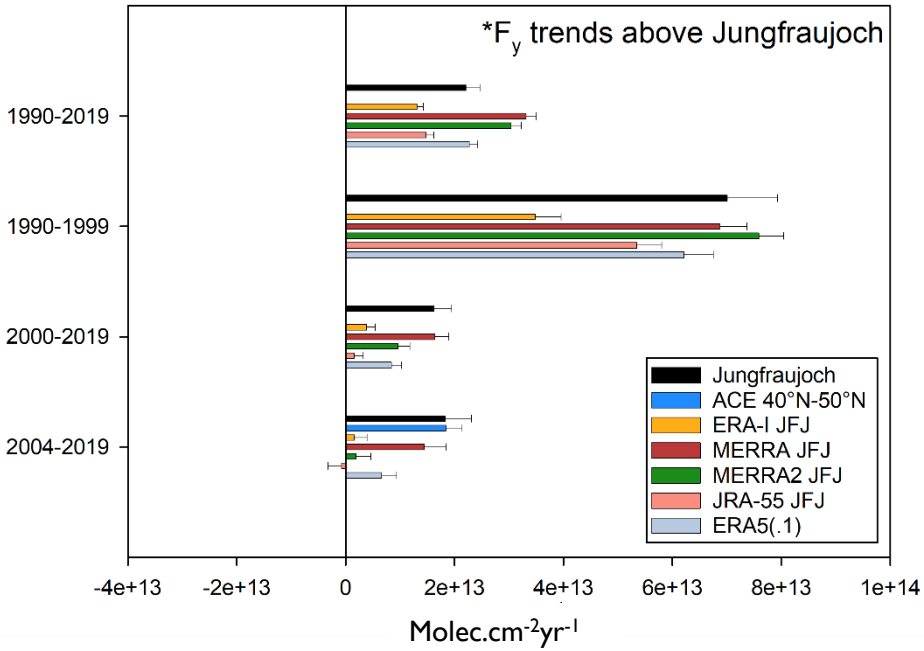

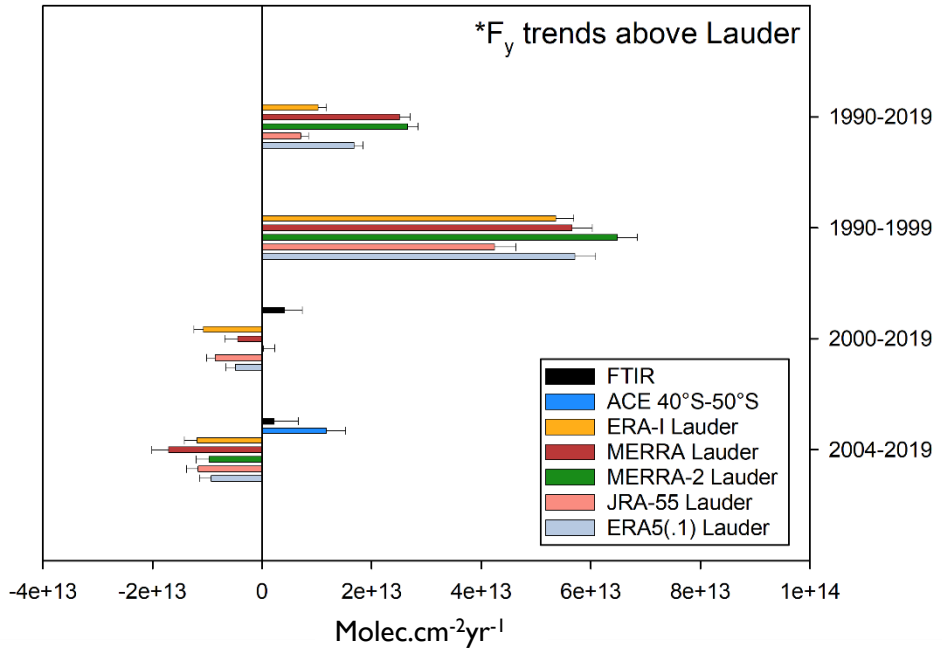

Long-term trends

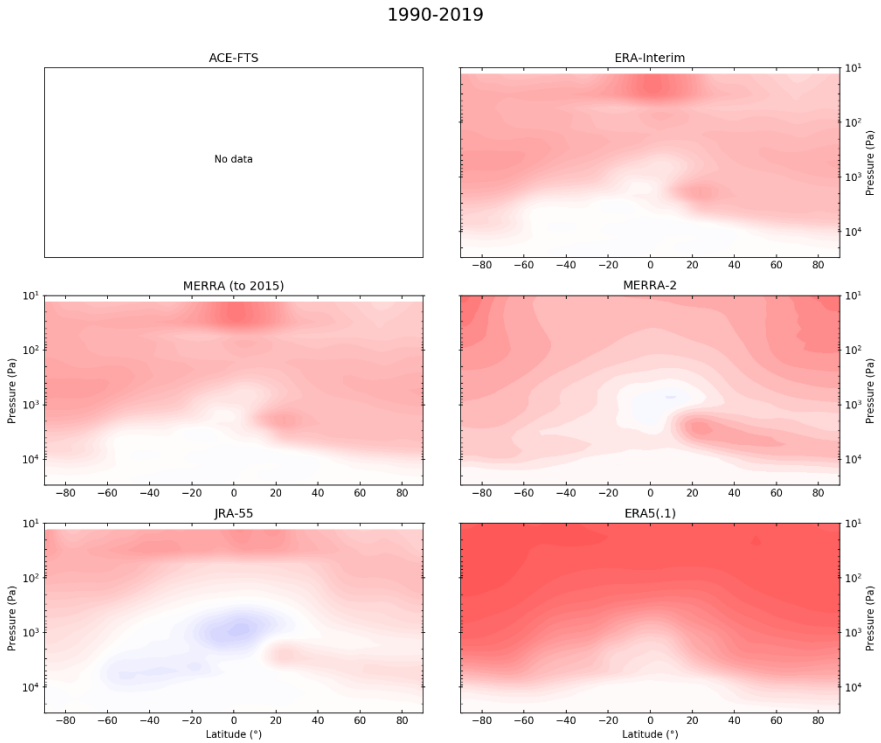

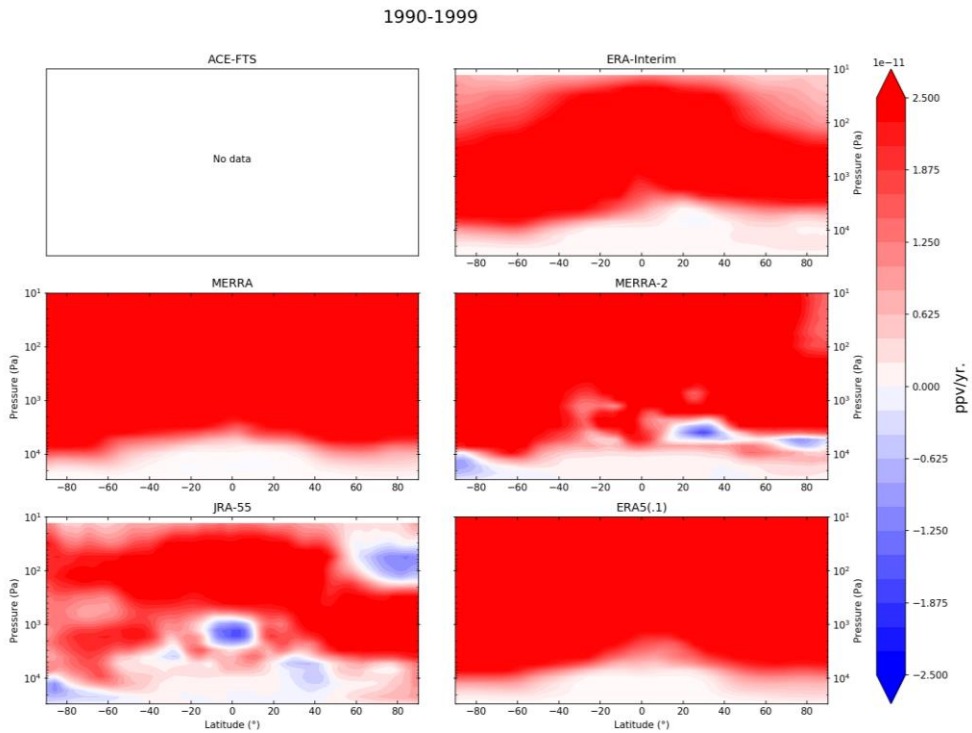

Long-term trends

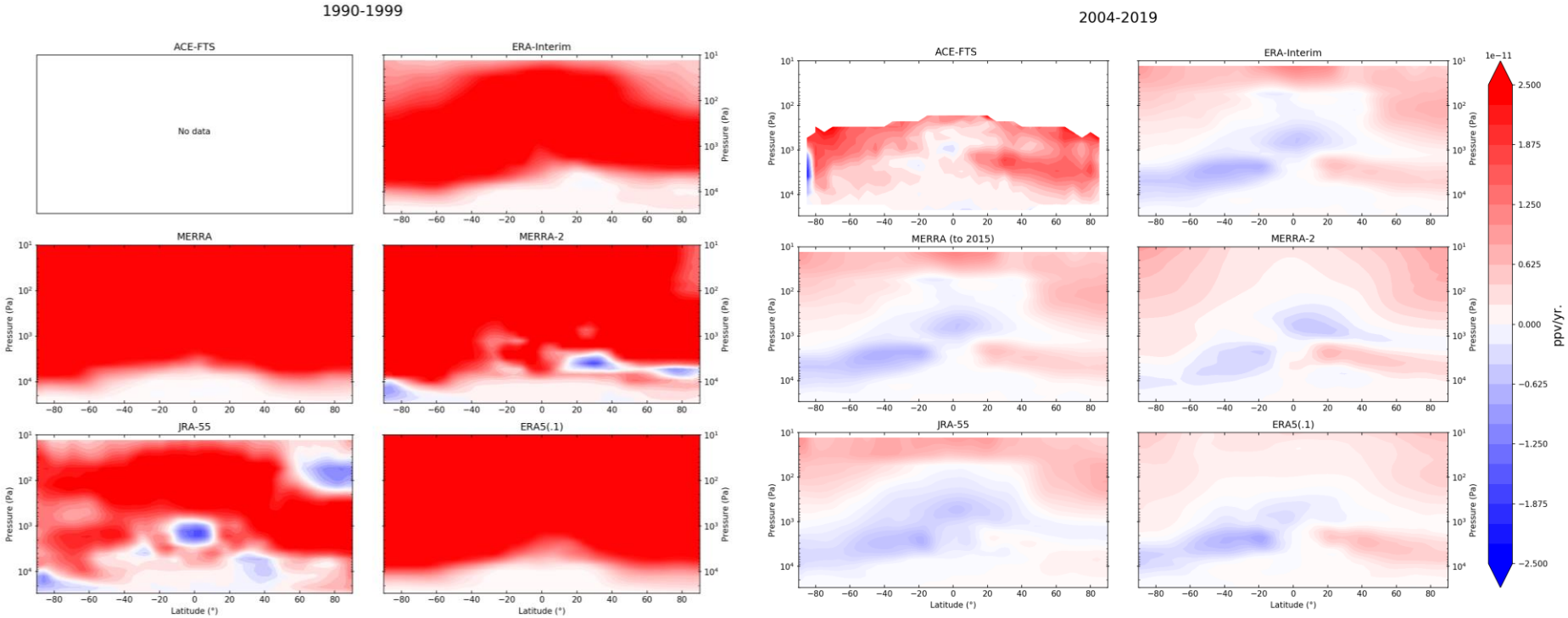

Short-term trends

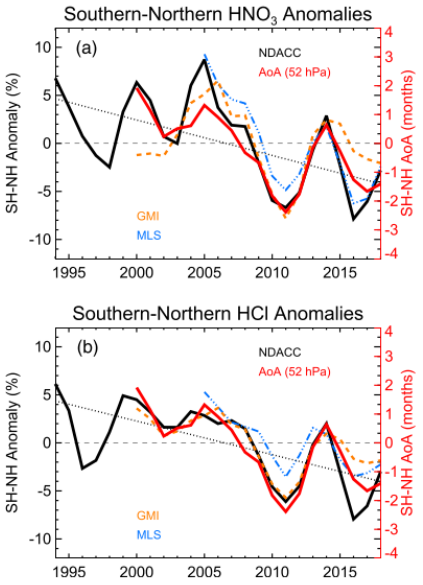

Figure 3. NDACC (black), MLS (blue), and GMI (orange) interhemispheric difference (Southern Hemisphere – Northern Hemisphere) for (a) HNO_3 and (b) HCl anomaly time series. The IH difference of GMI CTM age of air at 52 hPa (red) is plotted in each panel (see the right axis). The dashed line shows the linear trend for the NDACC anomalies. The trends and their uncertainties are reported in Table 1.

Strahan et al., GRL, 2020

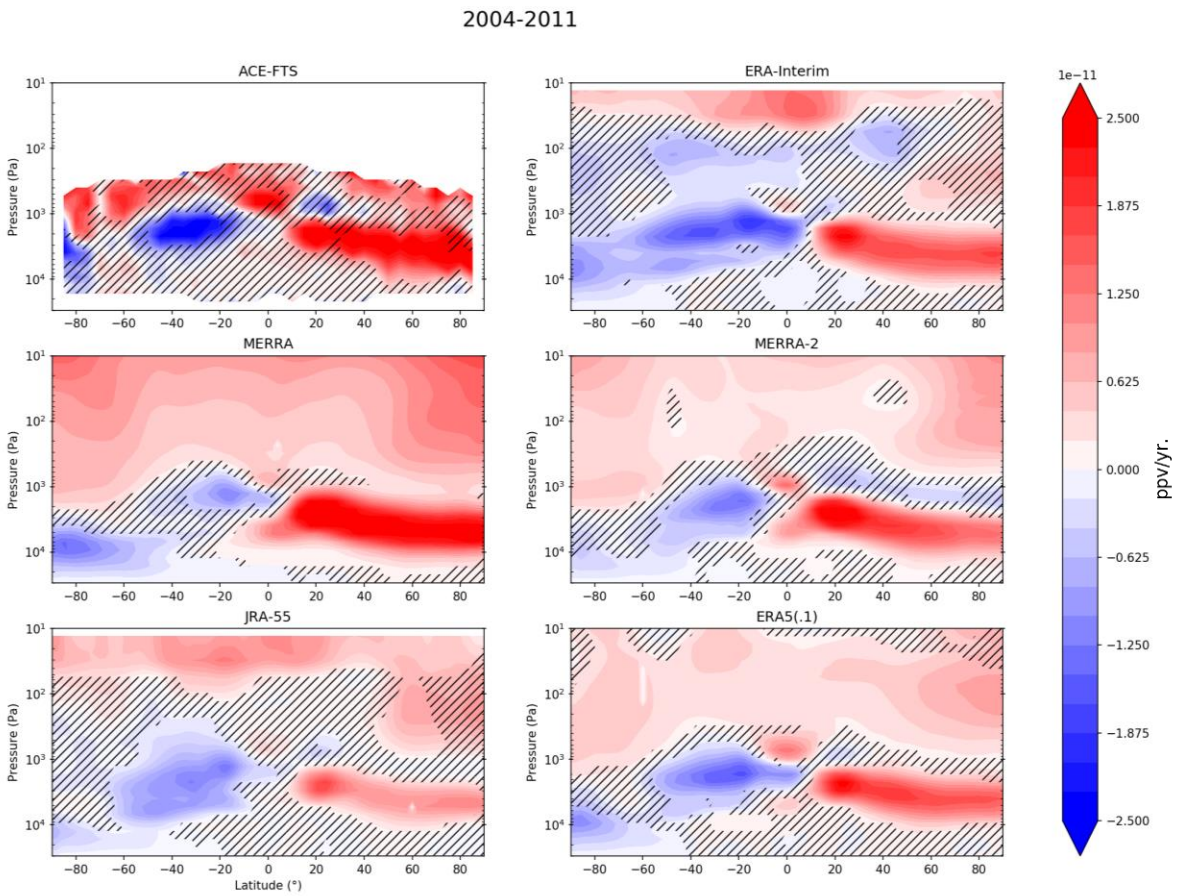

Jungfraujoch: $(3.23 \pm 0.85)e^{+13}$ molec.cm^{-2}yr^{-1}

Lauder: $(-0.43 \pm 1.53)e^{+13}$ molec.cm^{-2}yr^{-1}

Short-term trends

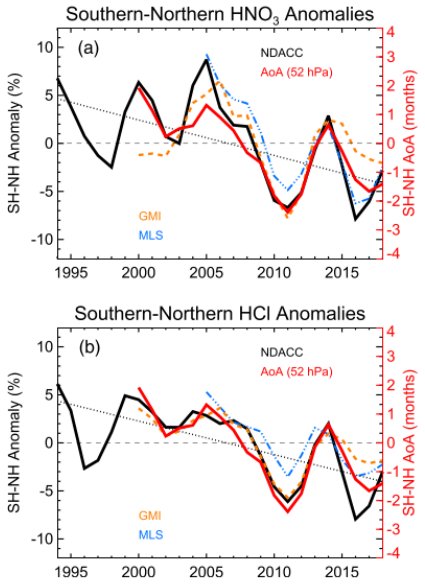

Figure 3. NDACC (black), MLS (blue), and GMI (orange) interhemispheric difference (Southern Hemisphere – Northern Hemisphere) for (a) HNO_3 and (b) HCl anomaly time series. The IH difference of GMI CTM age of air at 52 hPa (red) is plotted in each panel (see the right axis). The dashed line shows the linear trend for the NDACC anomalies. The trends and their uncertainties are reported in Table 1.

Strahan et al., GRL, 2020

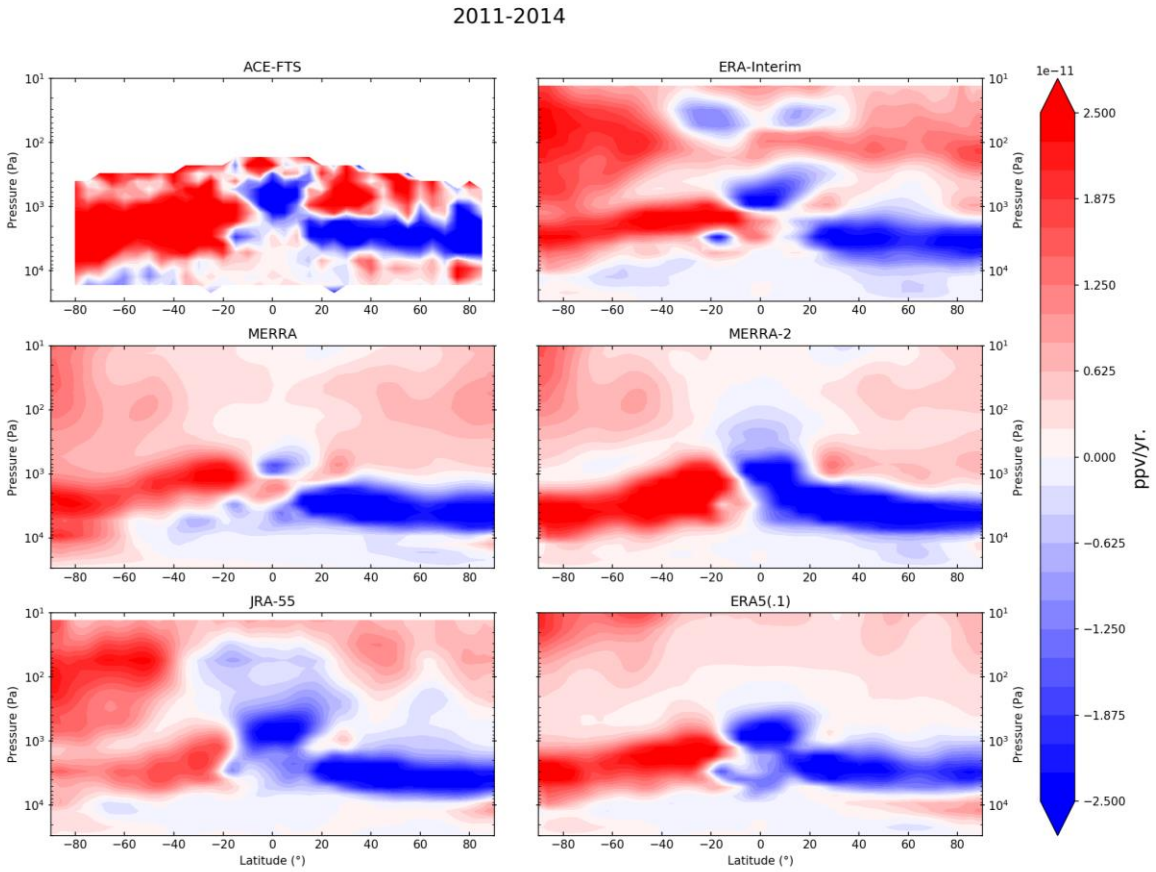

Jungfraujoch: $(-2.63\pm2.67)e^{+13}$ molec.cm^{-2}yr^{-1}
Lauder: $(4.31\pm3.60)e^{+13}$ molec.cm^{-2}yr^{-1}